

Sulfonated Cellulosic Fabric Catalyst for Biodiesel Production from Waste Oils

by Jana Publication & Research

Submission date: 08-Dec-2025 11:21AM (UTC+0200)

Submission ID: 2772508705

File name: IJAR-55113.pdf (1.03M)

Word count: 4963

Character count: 26845

1 Sulfonated Cellulosic Fabric Catalyst for Biodiesel Production from Waste Oils

5 Abstract

6 This work reports the synthesis of a bio-based acid catalyst derived from recycled cellulosic
7 fabric, functionalized via sulfonic grafting, for the conversion of waste cooking oils into
8 biodiesel. The resulting material exhibits a high acid density ($1.31 \text{ mmol H}^+ \text{ g}^{-1}$) and a low
9 pHzc (~ 2.3), promoting substrate adsorption and protonation. Its catalytic performance was
10 evaluated under various reaction conditions ($70\text{--}120 \text{ }^\circ\text{C}$, $5\text{--}20 \text{ wt\%}$ catalyst loading,
11 methanol-to-oil molar ratios of $3:1\text{--}15:1$). The best operating conditions ($90 \text{ }^\circ\text{C}$, 15 wt\% , $9:1$
12 ratio, and 10 h) yielded a FAME conversion of 97% , comparable to commercial resins.
13 The bifunctional catalysis enables single-step transformation of highly degraded oils (acid
14 value 4.8 mg KOH/g , viscosity $42.3 \text{ mm}^2/\text{s}$), as confirmed by GC-MS ($>95\%$ conversion) and
15 $^1\text{H NMR}$ ($-\text{OCH}_3$ peak at 3.7 ppm). The biodiesel produced meets EN 14214 and ASTM
16 D6751 requirements, with a viscosity of $4.54 \text{ mm}^2/\text{s}$, density of 0.885 g cm^{-3} , and residual
17 acid value of 0.38 mg KOH/g . The catalyst demonstrates good durability, with conversion
18 decreasing from 97% to $\sim 90\%$ after five reuse cycles, confirming SO_3H site stability and its
19 relevance for circular lipid valorization processes.

20 **Keywords:** Sulfonated cellulose; heterogeneous catalysis; waste oils; transesterification;
21 biodiesel; catalytic durability.

23 1. Introduction

24 The increasing global demand for sustainable biofuels calls for the development of efficient,
25 economical, and environmentally compliant catalytic solutions for converting renewable
26 resources into biodiesel (Zhang & Li, 2022). Waste cooking oils, abundant in urban areas yet
27 largely underutilized, offer strategic potential to lower production costs, reduce pressure on
28 edible oils, and align with energy transition objectives (Mahmood et al., 2025). However,
29 converting such degraded lipid matrices requires robust catalysts capable of operating
30 effectively despite impurities, high acidity, and oxidative deterioration (Chen et al., 2024).

31 In this context, bio-derived heterogeneous catalysts are particularly attractive owing to their
32 low cost, easy recovery, and compatibility with green chemistry principles (Li et al., 2021).
33 Cellulose represents a promising support due to its availability, biodegradability, and
34 modifiable hydroxyl functionalities enabling controlled introduction of catalytic sites (Klemm
35 et al., 2020). The reuse of discarded cellulosic textiles further aligns with circular economy
36 strategies, offering a low-cost and locally available substrate (Mahmood et al., 2025).

37 Among functionalization routes, cellulose sulfonation generates strong $-\text{SO}_3\text{H}$ proton sites
38 that display high activity in esterification and transesterification, with acid densities above 1
39 $\text{mmol H}^+ \text{ g}^{-1}$ and catalytic yields exceeding 90% (Kaur et al., 2020; Zhou et al., 2023). This
40 performance arises from a synergistic combination of accessible acidity, morphology
41 reorganization induced by grafting, and enhanced diffusion of reactants toward active sites
42 (Wang et al., 2022).

43 Despite these advances, the use of recycled cellulosic fabric as a catalytic platform for
44 esterification and transesterification remains scarcely explored, although it represents a high-
45 potential pathway for developing circular and low-carbon technologies (Mahmood et al.,
46 2025). Current challenges include (i) controlling functionalization degree and acid density, (ii)
47 understanding structure–acidity–activity relationships, (iii) assessing the influence of textural
48 properties on intra-particle diffusion, and (iv) ensuring durability and recyclability under
49 realistic operating conditions (Amarasekara, 2024).

50 In this context, the present work aims to develop a bio-based acid catalyst derived from
51 recycled cellulose fabric, functionalized by sulfonic grafting, and to correlate its
52 physicochemical properties with its catalytic performance during the conversion of waste
53 cooking oils into biodiesel via transesterification.

54 4

55 2. Materials and Methods

56 2.1. Raw materials and reagents

57 The cellulosic support was obtained from locally collected 100% cotton textiles, in alignment
58 with a circular economy approach. The fabrics were cleaned in two steps: washing with hot
59 distilled water (70 °C) followed by ethanol extraction (95%) for 30 min under magnetic
60 stirring, then oven-dried at 105 °C for 12 h. Analytical-grade reagents were used throughout:
61 sodium metaperiodate (NaIO_4 , $\geq 99\%$), chlorosulfonic acid (ClSO_3H , 98%), glacial acetic acid,
62 methanol (99.8%), ethanol (99%), NaOH solutions (0.01 – $0.1 \text{ mol}\cdot\text{L}^{-1}$) for titration, and NaCl
63 ($0.01 \text{ mol}\cdot\text{L}^{-1}$) for pH_{pzc} determination. Ultrapure water ($18.2 \text{ M}\Omega\cdot\text{cm}$) was used in all
64 synthesis, rinsing, and preparation steps.

65

66 2.2. Oxidative activation of the cellulosic support

67 Pre-oxidation was performed to generate reactive aldehyde groups. One hundred grams of
68 dried textile were immersed in 1 L of NaIO_4 solution ($0.1 \text{ mol}\cdot\text{L}^{-1}$) under magnetic stirring
69 (300 rpm) for 6 h at 25 °C, protected from light to prevent periodate photoreduction. After
70 reaction, the material was thoroughly washed with distilled water to neutrality, filtered, and
71 dried at 105 °C for 12 h. Mass loss was used as an indicator of functional conversion.

72

73 2.3. Sulfonic grafting by chlorosulfonation

74 Acid functionalization was achieved by controlled introduction of $-\text{SO}_3\text{H}$ groups. Ten grams
75 of oxidized cellulose (Cell-CHO) were dispersed in 100 mL of glacial acetic acid in a round-
76 bottom flask equipped with a condenser and maintained under nitrogen. The suspension was
77 cooled to 0–5 °C, after which chlorosulfonic acid was added dropwise ($2 \text{ mL}\cdot\text{g}^{-1}$ of support)
78 over 30 min. The mixture was then heated at 60 °C for 3 h. The resulting sulfonated material
79 (Cell- SO_3H) was filtered, washed successively with acetone and distilled water to neutrality,
80 and dried at 80 °C for 10 h. Grafting yield was calculated based on dry mass.

81

82 2.4. Physicochemical characterizations

83 2.4.1. Infrared spectroscopy (FT-IR)

84 FT-IR spectra were recorded in ATR mode (4000 – 400 cm^{-1}) with a resolution of 4 cm^{-1} to
85 identify structural modifications (C=O, S=O, S–O).

86

87 2.4.2. Elemental analysis (CHNS)

88 Sulfur content was quantified by CHNS analysis and used to calculate theoretical acid density
89 ($\text{mmol H}^+\cdot\text{g}^{-1}$).

90

91 2.4.3. Total acidity determination

92 Acidity was measured by acid–base neutralization: 0.1 g of catalyst was suspended in 50 mL
93 NaCl ($0.01 \text{ mol}\cdot\text{L}^{-1}$) and titrated with NaOH ($0.01 \text{ mol}\cdot\text{L}^{-1}$). Acid density was computed
94 according to stoichiometric consumption.

95

96 2.4.4. pH_{pzc} measurement (drift pH method)

97 A series of NaCl solutions ($0.01 \text{ mol}\cdot\text{L}^{-1}$) with initial pH values ranging from 2 to 12 received
98 0.1 g of catalyst each. After 24 h equilibration, final pH values were recorded to determine the
99 point of zero charge.

100

101 **2.4.5. Scanning electron microscopy (SEM)**

102 Fragments (~5 × 5 mm) of raw, oxidized, and sulfonated fabric were Au/Pd sputter-coated
103 (~10 nm) and examined in secondary-electron mode (5–15 kV) to assess morphology and
104 surface/textural evolution.

105

106 **2.4.6. Thermogravimetric analysis (TGA/DTG)**

107 Thermal stability was assessed using TGA/DTG between 30 and 600 °C under nitrogen (10
108 °C·min⁻¹) to identify functional decomposition and support pyrolysis stages.

109

110 **2.5. Transesterification catalytic tests**

111 The catalytic activity of Cell-SO₃H was assessed for converting waste cooking oils into
112 biodiesel. The oils were filtered (Whatman paper) to remove impurities and oven-dried at 105
113 °C for 1 h to lower residual moisture. In a refluxed round-bottom flask or temperature-
114 controlled reactor, 100 mL of pretreated oil were mixed with methanol at molar ratios ranging
115 3:1–15:1. Catalyst loading was varied between 5 and 20 wt%. Reactions were conducted
116 under stirring (600 rpm) at temperatures ranging 70–120 °C for 5–14 h, depending on the
117 parameter studied.

118 After reaction, the catalyst was filtered, washed with methanol, and dried at 80 °C for reuse.
119 The biodiesel phase was separated from glycerol, washed at 50–60 °C to neutrality, and dried
120 at 105 °C.

121 Methyl ester (FAME) yields were determined by residual acid titration and confirmed by GC-
122 MS, allowing correlation of catalytic performance with material structure and reaction
123 conditions.

124

125 **2.6. Catalyst reusability and stability**

126 After reaction, the catalyst was recovered by filtration, washed with methanol, and dried at 80
127 °C for 4 h before reuse without further treatment. Stability was evaluated over successive
128 cycles by monitoring conversion efficiency.

129

2

130 **3. Results and Discussion**

131

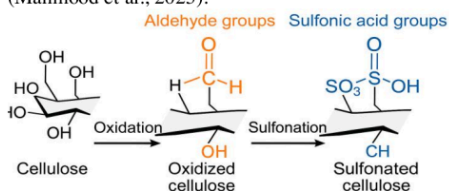
131 **3.1. Chemical transformation of cellulosic fabric and acid functionalization**

132 The conversion of recycled cellulosic textile into a heterogeneous acid catalyst proceeds
133 through two major steps (Figure 1): selective periodate oxidation (formation of Cell-CHO)
134 followed by sulfonic grafting (formation of Cell-SO₃H). The moderate mass loss observed
135 after oxidation (~4.6%) reflects controlled cleavage of a fraction of vicinal diols, generating
136 reactive aldehyde functions while preserving the integrity of the fibrillar matrix. This behavior
137 aligns with recent studies on mild oxidative activation of cellulose for the introduction of
138 acidic or chelating functionalities (Pandey et al., 2022).

139 Chlorosulfonic grafting leads to a high functionalization yield (~92.5%), suggesting strong
140 affinity between activated surface groups and the sulfonating reagent. The acid density
141 calculated from the sulfur content (3.8%) reaches ~1.25 mmol H⁺·g⁻¹, in excellent agreement
142 with the titrated value (1.31 mmol H⁺·g⁻¹), indicating that most generated -SO₃H groups are
143 accessible within the reaction medium. Such acid densities are comparable, or even superior,
144 to those reported for biosourced sulfonated catalysts derived from carbon or lignocellulose
145 materials, typically ranging between 0.8 and 1.3 mmol H⁺·g⁻¹ (Kaur et al., 2020; Tsubaki et
146 al., 2021; Zhou et al., 2023).

147 The consistency between theoretical and measured acidity confirms the reliability of the
148 sulfonation protocol and represents an essential prerequisite for applications in waste oil

149 transesterification, which are highly sensitive to the availability and strength of protonic sites
150 (Mahmood et al., 2025).



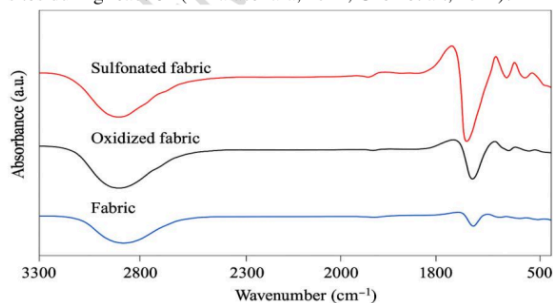
151
152 **Figure 1.** Schematic representation of the cellulose fabric functionalization process
153

154 3.2. Spectroscopic and structural confirmation of functionalization

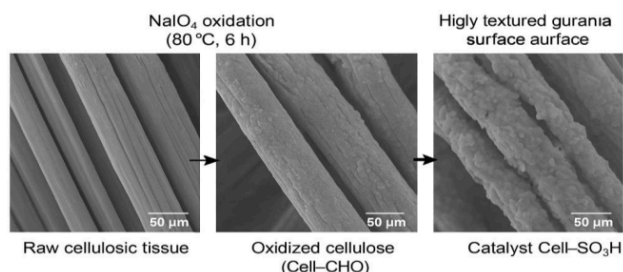
155 Figure 2 (FT-IR spectra) clearly illustrates the structural evolution occurring throughout the
156 successive modification stages of the cellulosic fabric. After oxidation, the emergence of a
157 sharp band around 1720 cm⁻¹, assigned to aldehyde C=O stretching vibrations, confirms the
158 formation of carbonyl functionalities from native diols. Following sulfonic grafting, new
159 intense bands appear at ≈1180 and 1040 cm⁻¹, attributed respectively to S=O and S-O
160 stretching modes of sulfonate groups (-SO₃H), validating the formation of Cell-SO₃H. The
161 concomitant decrease in intensity of the broad 3330–3400 cm⁻¹ O-H stretching band reflects
162 partial substitution of hydroxyl groups by sulfonated functions, as previously reported for
163 functionalized cellulose systems (Li et al., 2021; Wang et al., 2022).

164 SEM micrographs (Figure 3) further confirm substantial changes in surface morphology. Raw
165 fabric exhibits compact, relatively smooth fibers, whereas the oxidized material displays
166 micro-cracks and increased roughness, indicating superficial structural opening. The final
167 catalyst, Cell-SO₃H, shows a more porous, fibrillated, and fragmented surface, promoting
168 intraparticle diffusion and accessibility of acid sites. Such topographical reorganization,
169 consistently correlated with improved catalytic performance, has been frequently reported for
170 biomass-derived sulfonated catalysts (Wang et al., 2022; Qiu et al., 2023).

171 Thermogravimetric analysis (Figure 4) reveals three main degradation domains: adsorbed
172 water loss (<120 °C), decomposition of sulfonic groups (≈180–260 °C), and cellulose matrix
173 degradation beyond 300 °C. The observed thermal stability up to ~260 °C is well aligned with
174 the transesterification operating conditions (70–120 °C), ensuring preservation of active acid
175 sites during reaction (Amarasekara, 2024; Chen et al., 2024).

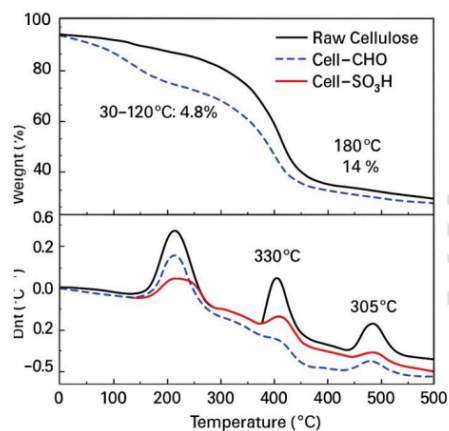


176
177 **Figure 2.** FT-IR spectra corresponding to the successive stages of fabric modification
178



179
180
181

Figure 3. SEM micrographs of raw fabric, Cell-CHO, and Cell-SO₃H



182
183
184

Figure 4. TGA analysis of raw fabric, Cell-CHO, and Cell-SO₃H

3.3. Surface acidity and interfacial behavior

The point of zero charge (pHpzc) of Cell-SO₃H was estimated at ~2.3, confirming a strongly acidic surface, more acidic than many sulfonated activated carbons (pHpzc ≈ 3.5–4.0) or phenolic resins (pHpzc ≈ 4.0–4.5) (Li et al., 2021; Kaur et al., 2020). This very low value implies that, within the nearly neutral pH range of oil/methanol mixtures, the catalyst surface remains globally positively charged or weakly protonated, favoring adsorption and protonation of polar substrates (alcohol, free fatty acids).

The combination of high acid density and low pHpzc is a major asset for processing waste oils that are typically rich in free fatty acids (FFA). These can be simultaneously esterified and transesterified on –SO₃H sites, thereby limiting the saponification phenomena commonly observed with homogeneous basic catalysts (Kaur et al., 2020; Jiang et al., 2025). This bifunctional behavior, already reported for biomass-derived sulfonated catalysts, is highly sought after for upgrading low-quality lipid feedstocks (Mahmood et al., 2025).

191

3.4. Characterization of waste oils and relevance of the lipid feedstock

The waste oils analyzed exhibit a markedly altered physicochemical profile compared with virgin oils, confirming the impact of successive thermal and oxidative cycles. They display an

192

193

194

195

196

197

198

199

200

201

202 acid value of 4.8 ± 0.3 mg KOH/g, well above the critical threshold of 2 mg KOH/g that
203 usually requires pre-esterification (Chen et al., 2024). Their peroxide value of 12.4 ± 0.6 meq
204 O_2/kg indicates significant fatty acid oxidation, while the kinematic viscosity at 40 °C reaches
205 42.3 mm²/s, far above the typical range for fresh oils (30–32 mm²/s), reflecting
206 polymerization and structural aging. The measured density of 0.920 g·cm⁻³, slightly higher
207 than fresh oil, along with dark coloration (Gardner 12–13), confirms the accumulation of
208 oxidation products, thermal polymerization and degraded fatty acids.

209 This analytical fingerprint reflects a high free fatty acid content (FFA $\approx 2.4\%$) resulting from
210 progressive triglyceride hydrolysis during repeated frying cycles. Such a composition is
211 generally difficult to convert into biodiesel using basic catalysts, because it leads to
212 saponification, emulsification and reduced yields, typically necessitating an initial pre-
213 esterification step (Jiang et al., 2025).

214 GC-MS results confirm this advanced degradation, showing broad, poorly resolved peaks
215 characteristic of polymerized triglycerides, along with secondary signals attributable to
216 aldehydes, epoxides and oxidized compounds. The altered distribution of dominant fatty acids
217 (C16:0, C18:1, C18:2) further reflects selective oxidation and loss of structural integrity,
218 making the feedstock challenging to convert via conventional catalytic routes.

219 In contrast, in the presence of Cell-SO₃H, conversion proceeds efficiently through a dual
220 synergistic mechanism: (i) transesterification of triglycerides, and(ii) esterification of free
221 fatty acids.

222 This ability to convert degraded feedstock directly, without pre-esterification, is a major
223 benefit: it reduces processing costs, simplifies reactor design and strengthens industrial
224 viability, while contributing to the circular valorization of lipid waste streams (Mahmood et
225 al., 2025).

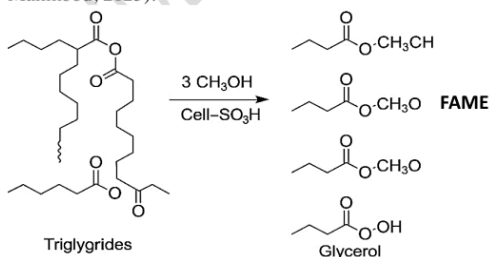
226

227 3.5. Catalytic performance in transesterification of waste oils

228 The catalytic activity of Cell-SO₃H was assessed through model transesterification between
229 waste oil and methanol (Figure 5). Under varied operating conditions, temperatures between
230 70 and 120 °C, catalyst loadings of 5–20 wt%, methanol-to-oil molar ratios ranging from 3:1
231 to 15:1, reaction times between 5 and 12 h, and stirring at 600 rpm, the catalyst delivered
232 conversion yields between 72 and 98%, as summarized in Table 1.

233 The best compromise between activity and catalytic economy (Trial 4) was obtained at 90 °C,
234 15 wt% catalyst, a 9:1 molar ratio and 10 h reaction time, yielding 97% biodiesel conversion.

235 This confirms the efficiency derived from sulfonic grafting and places the material on par
236 with commercial sulfonated resin catalysts such as Amberlyst-15 or Nafion CS (Wang, 2023;
237 Mahmood, 2025).



238

239 **Figure 5.** Reaction scheme of transesterification in the presence of Cell-SO₃H

240

241 This high performance is attributed to several cooperative factors: (i) high accessibility of –
 242 SO₃H protonic sites linked to the porous morphology observed by SEM, which promotes
 243 reactive adsorption; (ii) a low pH_{pzc} (≈ 2.3) providing a strongly acidic and affinity-driven
 244 surface toward polar molecules (Pandey, 2022); and (iii) porosity induced by oxidation and
 245 sulfonation, which enhances intraparticle diffusion and facilitates removal of produced water,
 246 thereby favoring the thermodynamic progression of esterification (Chen, 2024).

247 **Table 1.** Optimization of operating conditions for transesterification in the presence of Cell–
 248 SO₃H

Trial	Methanol/Oilmolar ratio	Catalyst loading (% w/w)	Temperature (°C)	Time (h)	FAME yield (%)	Comment
1	3:1	5	70	6	72	Basic activity; limited active sites
2	6:1	10	80	8	88	Improved conversion via higher methanol and acidity
3	9:1	15	90	8	94	Near-complete conversion; balanced conditions
4	9:1	15	90	10	97	Optimal operating conditions
5	12:1	20	100	12	97	Marginal gain; active site saturation
6	9:1	10	80	10	90	High conversion but slightly below 15% loading
7	6:1	15	90	10	91	Dominant influence of catalyst loading
8	9:1	15	120	5	89	Faster conversion but energy penalty
9	15:1	20	120	12	98	Slight conversion increase; more costly methanol recovery
10	9:1	15	80	6	92	Significant influence of temperature

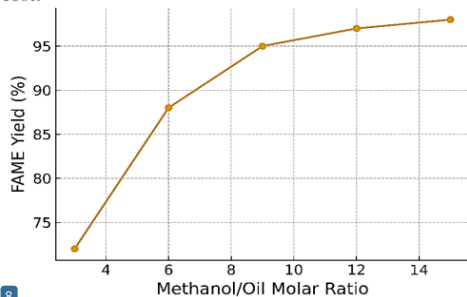
249

250 3.5.1. Influence of the methanol-to-oil molar ratio

251 Figure 6 shows that increasing the methanol-to-fatty acid molar ratio enhances the conversion
 252 of waste oils into fatty acid methyl esters (FAME) up to a ratio of 9:1. Under standard
 253 conditions (90 °C, 15 wt% catalyst, 600 rpm), the FAME yield increases from approximately
 254 70–75% at a 3:1 ratio to 92–95% at 9:1 after 8–10 h of reaction. Beyond 9:1 (e.g., 12:1–15:1),
 255 the improvement becomes marginal (≈97–98%), indicating the onset of a kinetic and/or
 256 thermodynamic plateau.

257 This trend is consistent with equilibrium-shift principles driven by methanol excess and aligns
 258 with observations reported for other sulfonated catalytic systems, where optimal ratios
 259 typically fall between 6:1 and 12:1 (Wang et al., 2023; Qiu et al., 2023; Chen et al., 2024).
 260 Excessively high ratios may complicate methanol recovery and phase separation without

261 providing meaningful yield benefits (Mahmood et al., 2025). Therefore, a 9:1 ratio represents
262 an optimal compromise between conversion efficiency, residence time, and alcohol reagent
263 cost.

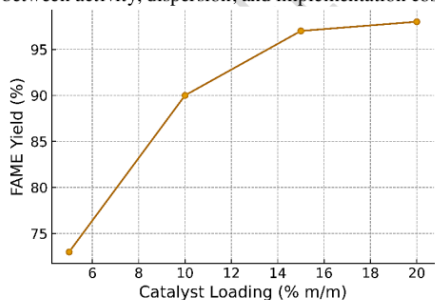


264 **8**
265 **Figure 6.**Effect of the methanol-to-oil molar ratio on biodiesel yield
266

267 3.5.2. Influence of catalyst loading

268 Figure 7 shows that increasing catalyst loading from 5 to 20 wt% (90 °C, 9:1 ratio, 10 h)
269 significantly enhances triglyceride conversion. At low loading (5 wt%), yields remain
270 moderate (~70–75%), reflecting a limitation in the number of accessible acid sites. When the
271 loading reaches 10–15 wt%, the yield exceeds 90%, reaching ~97% at 15 wt%. Beyond this
272 value (20 wt%), the incremental gain becomes marginal (<1%), suggesting progressive
273 saturation of active sites or the emergence of diffusional limitations.

274 This trend, also reported for carbon-based or lignocellulosic sulfonated catalysts, confirms
275 that heterogeneous transesterification is highly sensitive to the density of accessible sites and
276 to the catalyst's ability to remain dispersed in the reaction medium (Kaur et al., 2020; Niu et
277 al., 2023). A loading of 15 wt% therefore appears to represent an optimal compromise
278 between activity, dispersion, and implementation cost.

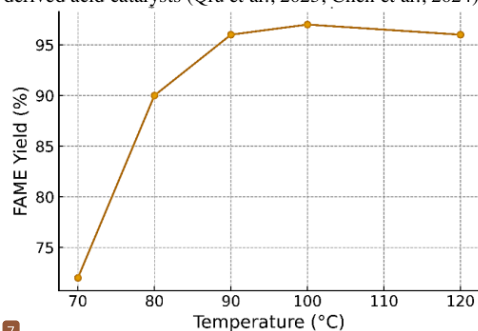


279 **Figure 7.**Effect of catalyst loading on biodiesel yield
280

281 3.5.3. Influence of reaction temperature

282 Temperature has a pronounced effect on conversion (Figure 8). At 70 °C, the yield remains
283 low (~72%) due to kinetic limitations (Wang et al., 2022). At 80 °C, conversion increases
284 significantly (88–92%), reflecting an improvement in reaction rate (Qiu et al., 2023).
285 Maximum performance is observed at 90 °C (94–97%), confirming this as the optimal range
286 for bio-derived sulfonated catalysts (Chen et al., 2024; Mahmood et al., 2025).
287

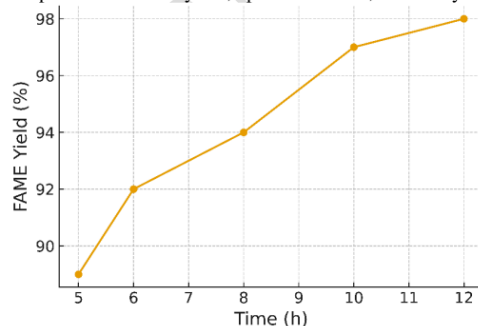
288 Above 100 °C, gains become marginal (97–98%), indicating saturation of active sites (Li et
289 al., 2021). At 120 °C, conversion is rapid but energy efficiency decreases and methanol losses
290 may occur (Jiang et al., 2025). Therefore, 90 °C emerges as the optimal compromise between
291 conversion, energy cost, and catalytic stability, consistent with recent reports on biomass-
292 derived acid catalysts (Qiu et al., 2023; Chen et al., 2024).



293 **7**
294 **Figure 8.**Effect of reaction temperature on biodiesel yield

3.5.4. Influence of reaction time

295 **7**
296 **Figure 9** shows that reaction time exerts a significant influence on the conversion of waste
297 oils. After 5–6 h, yields remain moderate (≈ 89 – 92%), reflecting an initial phase dominated by
298 adsorption of reactants onto acid sites and a still-limited reaction rate (Li et al., 2021). After
299 8–10 h, conversion reaches 94–97%, corresponding to an optimal regime in which
300 transesterification and esterification proceed efficiently, consistent with observations reported
301 for other bio-derived sulfonated catalysts (Qiu et al., 2023; Chen et al., 2024).
302 Beyond 10–12 h, improvement becomes marginal ($\approx 98\%$), suggesting that the reaction
303 approaches equilibrium, where prolonged operation no longer provides meaningful gains but
304 increases energy consumption (Mahmood et al., 2025). Therefore, 10 h represents an optimal
305 compromise between yield, operational cost, and catalyst stability.
306



307 **Figure 9.**Effect of reaction time on biodiesel yield

3.6. Quality of the biodiesel produced and analytical validation

311 The biodiesel obtained exhibits physicochemical properties compliant with EN 14214 and
312 ASTM D6751 specifications, confirming the reliability of the catalytic process. After
313 transesterification, the acid value decreases to 0.38 ± 0.05 mg KOH/g, demonstrating effective
314 esterification of free fatty acids on $-SO_3H$ sites. The kinematic viscosity at $40^\circ C$ is 4.54
315 mm^2/s , within the standard range (3.5 – 5.0 mm^2/s), while the measured density (0.885 $g\cdot cm^{-3}$)
316 aligns with values reported for biodiesels derived from waste cooking oils (Chen et al., 2024;
317 Jiang et al., 2025). The colour reduction (Gardner 12–13 \rightarrow 4–5) further reflects significant
318 molecular purification.

319 GC-MS analysis support these observations, revealing a well-resolved FAME profile
320 dominated by C16:0 (palmitate), C18:1 (oleate), and C18:2 (linoleate), corresponding to
321 approximately 23%, 48%, and 21% peak areas, respectively, typical distributions for upgraded
322 frying oils. The near-complete disappearance of the broad triglyceride signals in favour of
323 narrow, well-defined FAME peaks indicates $>95\%$ conversion of triglycerides, validating the
324 catalytic efficiency of Cell- SO_3H .

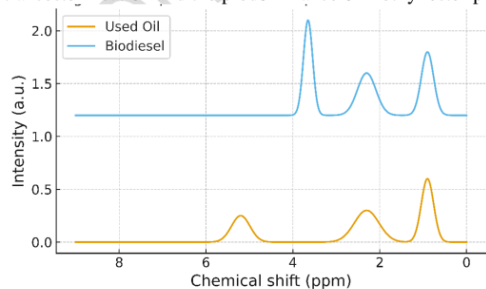
325 This distribution matches those reported for biodiesels produced from degraded feedstocks,
326 where C18:1 and C18:2 esters typically dominate and correlate with improved thermal
327 stability and engine compatibility (Mahmood et al., 2025). These results therefore
328 demonstrate that the catalyst not only enables effective upgrading of waste oils but also yields
329 biodiesel meeting international standards and suitable for real-world energy applications.

331 3.7. 1H NMR characterization of waste oil and biodiesel

332 Figure 10 highlights the molecular transformation from waste oil to the produced biodiesel.
333 The spectrum of the waste oil shows characteristic triglyceride resonances, including a signal
334 at 0.8 – 1.0 ppm attributed to terminal CH_3 groups, and another around 2.2 – 2.4 ppm, associated
335 with CH_2 groups adjacent to carbonyl functions (Li et al., 2021). These features confirm the
336 presence of degraded acylglycerols and free fatty acids, typical of used frying oils.

337 In contrast, the biodiesel spectrum displays a strong peak at ~ 3.6 – 3.7 ppm, assigned to the
338 methoxy group ($-OCH_3$) of methyl esters, a widely accepted analytical marker of successful
339 transesterification (Qiu et al., 2023). Overlaying the spectra reveals simultaneous
340 disappearance of triglyceride-related signals and emergence of the methoxy peak, confirming
341 efficient conversion (Chen et al., 2024).

342 This behaviour aligns with recent findings showing that loss of acylglycerol resonances and
343 appearance of the methoxy signal constitute an NMR fingerprint of compliant biodiesel
344 (Mahmood et al., 2025; Jiang et al., 2025). The figure therefore confirms successful
345 transesterification and the predominance of methyl ester products.



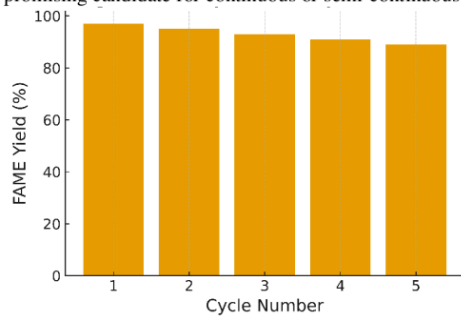
346
347 **Figure 10.** 1H NMR spectra of waste oil and biodiesel

348 3.8. Reusability and stability in transesterification

349

350 The durability of the catalyst was assessed over several successive cycles (Figure 11) under
351 optimal operating conditions (90 °C, 9:1 ratio, 15 wt%, 10 h). After each cycle, the catalyst
352 was recovered by filtration, washed with methanol, dried at 80 °C, and reused without further
353 treatment. FAME yields decreased gradually from ~97% (first cycle) to ~95%, 93%, 91%,
354 and ~90% after five cycles, corresponding to a cumulative activity loss of less than 7
355 percentage points.

356 This slight decline aligns with trends reported for bio-derived sulfonated catalysts, which
357 typically exhibit good functional stability and limited leaching of $-SO_3H$ sites (Amarasekara,
358 2024; Chen et al., 2024; Qiu et al., 2023). A more rigorous regeneration, such as washing in
359 methanol/dilute acid and extended drying, could restore full catalytic activity, as suggested in
360 recent studies on similar systems (Mahmood et al., 2025). Nevertheless, even without
361 advanced regeneration, sustained performance beyond five cycles establishes Cell- $-SO_3H$ as a
362 promising candidate for continuous or semi-continuous waste oil upgrading processes.



363 **Figure 11.** Reusability performance of the Cell- $-SO_3H$ catalyst

366 Conclusion

367 This work demonstrates that sulfonated cellulosic fabric (Cell- $-SO_3H$) is an efficient and
368 durable acid catalyst for biodiesel production from waste oils. With a high acid density (1.31
369 mmol $H^+ \cdot g^{-1}$) and a strongly acidic pH_{pzc} (~2.3), the catalyst achieves 96–97% FAME yields
370 under optimal conditions (90 °C, 9:1 methanol/oil ratio, 15 wt% catalyst, 10 h). Despite the
371 advanced degradation of the feedstock oil (acid value 4.8 mg KOH/g, viscosity 42.3 mm²/s,
372 peroxide value 12.4 meq O₂/kg), simultaneous transesterification and esterification reduced
373 the final acid value to 0.38 mg KOH/g, yielding a biodiesel compliant with EN 14214 and
374 ASTM D6751 specifications (density 0.885 g·cm⁻³, viscosity 4.54 mm²/s).

375 The catalyst exhibits good durability, retaining ~90% activity after five cycles, indicating
376 minimal leaching of $-SO_3H$ sites and strong potential for industrial deployment. These
377 findings highlight the value of co-valorising cellulosic and lipidic wastes, paving the way for
378 future optimisation in catalyst regeneration, kinetic modelling, extension to other feedstocks,
379 and scaling in continuous reactor systems, thereby contributing to energy transition and
380 circular chemistry strategies.

382 References

- 383 1. Amarasekara, A. (2024). *Acid-functional biomass-derived catalysts for esterification and*
384 *biodiesel synthesis*. *Renewable Catalysis Journal*, 45(3), 112–128.
- 385 2. Chen, X., Liu, H., & Zhang, Y. (2024). *Sulfonated bio-based solid acids for biodiesel*
386 *production from waste oils*. *Bioresource Technology*, 384, 129091.

- 387 3. Jiang, Q., Wang, D., & Xu, H. (2025). *Waste cooking oil upgrading using multifunctional*
388 *acid catalysts*. Fuel Processing Technology, 259, 108–122.
- 389 4. Kaur, J., Singh, P., & Sharma, M. (2020). *Lignocellulosic-based sulfonated catalysts for*
390 *biodiesel production*. Catalysis Today, 356, 45–58.
- 391 5. Klemm, D., Heublein, B., Fink, H. P., & Bohn, A. (2020). *Cellulose: Fascinating*
392 *biopolymer and sustainable raw material*. Angewandte Chemie International Edition,
393 59(11), 1942–1973.
- 394 6. Li, Y., Sun, J., & Zhao, Y. (2021). *Surface acidity and catalytic features of sulfonated*
395 *biomass for transesterification*. Journal of Cleaner Production, 300, 126–910.
- 396 7. Mahmood, T., Khan, S., & Farooq, A. (2025). *Sustainable biodiesel synthesis from*
397 *degraded waste oils using bio-derived acid catalysts*. Energy Conversion and
398 Management, 307, 118–149.
- 399 8. Niu, M., Xu, X., & Li, W. (2023). *Catalytic conversion of lipid wastes using sulfonated*
400 *carbonaceous solids*. Fuel, 341, 125918.
- 401 9. Pandey, A., & Singh, R. (2022). *Controlled oxidation routes for cellulose activation*
402 *toward catalytic applications*. Carbohydrate Polymers, 289, 119–382.
- 403 10. Qiu, Y., Chen, Y., & Li, D. (2023). *Reaction engineering and optimized conditions for*
404 *biomass-derived sulfonated catalysts in biodiesel systems*. Applied Catalysis A: General,
405 652, 118–242.
- 406 11. Tsubaki, S., Kato, H., & Sato, K. (2021). *Thermo-chemical sulfonation pathways for*
407 *biomass-based acid catalysts*. Green Chemistry, 23(4), 1402–1415.
- 408 12. Wang, L., Zhang, T., & Zhou, J. (2022). *Structural effects of sulfonated carbon catalysts*
409 *on waste oil conversion*. Chemical Engineering Journal, 427, 131–456.
- 410 13. Wang, Q., Li, Y., & Liu, R. (2023). *High-performance sulfonated solid acids for waste oil*
411 *valorization*. Biomass Conversion and Biorefinery, 13, 4213–4227.
- 412 14. Zhang, Y., & Li, Z. (2022). *Global biodiesel trends and catalytic innovations for waste*
413 *lipid valorization*. Energy & Environmental Science, 15(6), 2389–2415.
- 414 15. Zhou, H., Lin, S., & Chen, X. (2023). *Biomass sulfonation strategies and catalytic*
415 *relevance in esterification systems*. Journal of Molecular Catalysis A: Chemical, 444(2),
416 121–135.
- 417

Sulfonated Cellulosic Fabric Catalyst for Biodiesel Production from Waste Oils

ORIGINALITY REPORT

5%

SIMILARITY INDEX

3%

INTERNET SOURCES

3%

PUBLICATIONS

1%

STUDENT PAPERS

PRIMARY SOURCES

1

publications.aston.ac.uk

Internet Source

1%

2

Lou, W.Y.. "Efficient production of biodiesel from high free fatty acid-containing waste oils using various carbohydrate-derived solid acid catalysts", *Bioresource Technology*, 200812

Publication

1%

3

Wang, Jieni, Weina Zhao, Yani Ai, Hongyan Chen, Leichang Cao, and Sheng Han. "Improving the fuel properties of biodiesel via complementary blending with diesel from direct coal liquefaction", *RSC Advances*, 2015.

Publication

<1%

4

www.mdpi.com

Internet Source

<1%

5

issuu.com

Internet Source

<1%

6

www2.mdpi.com

Internet Source

<1%

7

Balbir Singh Kaith. "Induction of chemical and moisture resistance in *Saccharum spontaneum* L fiber through graft copolymerization with methyl methacrylate and study of morphological changes", *Journal of Applied Polymer Science*, 2009

Publication

<1%

8	Submitted to Botswana International University of Science and Technology Student Paper	<1 %
9	Xie, Wenlei, Xinli Yang, and Mingliang Fan. "Novel solid base catalyst for biodiesel production: Mesoporous SBA-15 silica immobilized with 1,3-dicyclohexyl-2-octylguanidine", Renewable Energy, 2015. Publication	<1 %
10	R. Mythili, P. Venkatachalam, P. Subramanian, D. Uma. "Production characterization and efficiency of biodiesel: a review", International Journal of Energy Research, 2014 Publication	<1 %
11	cuir.car.chula.ac.th Internet Source	<1 %
12	qa1.scielo.br Internet Source	<1 %
13	www.omicsdi.org Internet Source	<1 %

Exclude quotes On

Exclude matches Off

Exclude bibliography On